Impact Factor (QJIF): 8.47 E-ISSN: 2583-1615, P-ISSN: 3049-3498

International Journal of Research in Academic World

Received: 24/May/2026 **IJRAW:** 2026; 5(8):13-17 **Accepted:** 28/June/2026

Cauchy's Mathematical Formulations on Thermoelasticity and Analytical Solutions to Pennes' Bioheat Transfer Equations in Living Human Tissues under Extreme Thermal Stress

[*1]Dr. Sangita B Pimpare

[*1]Associate Professor, NTVS's G.T. Patil Arts, Commerce and Science College Nandurbar, Maharashtra, India.

Abstract

This paper presents a rigorous study of thermal stresses induced within biological human tissue during exposure to severe external thermal environments. Drawing directly from Cauchy's fundamental stress principles and the generalized equations of thermoelasticity, we map how thermal gradients translate into structural mechanical loading within living tissue systems. To describe the underlying spatiotemporal temperature distribution, we apply the classical Pennes' Bioheat Transfer Equation (PBTE), which models tissue heat conduction alongside blood perfusion and metabolic heat generation. The mathematical governing equation is solved analytically using the method of separation of variables under standard physiological and boundary conditions. A complete mechanical analysis is then coupled to the thermal solution via Duhamel-Neumann constitutive relations to compute the induced Cauchy thermal stresses. Quantitative profiles indicate that rapid external heating creates highly localized, compressive thermal stress gradients near the skin surface, presenting a high risk for irreversible thermal injury. The results emphasize the critical role of blood perfusion as a thermal sink and pressure stabilizer.

Keywords: Bioheat Transfer, Pennes' Bioheat Equation, Cauchy Thermal Stress, Thermoelasticity, Thermal Stress.

Introduction

The study of heat transfer and subsequent mechanical deformation in biological systems—commonly referred to as bio-thermoelasticity—is vital to modern biomedical applications [1, 9]. When human skin or organ tissues are exposed to high-temperature fields (such as laser surgeries, hyperthermia cancer therapies, or extreme fire safety conditions), severe spatial temperature gradients develop rapidly [5, 10]. Because biological tissue is physically constrained by adjacent anatomical structures, non-uniform thermal expansion occurs, inducing significant internal mechanical forces known as thermal stresses [2].

Understanding the precise limits of these thermal stressors plays an instrumental role in clinical risk assessment. For instance, in laser dermatological ablation, precise modeling ensures targeted destruction of abnormal cells while safeguarding neighboring healthy tissue clusters [8, 14]. Similarly, in hyperthermia treatments designed to eradicate malignant tumor regions, maintaining a strict thermal threshold between 42°C and 45°C is paramount; exceeding this threshold causes rapid healthy tissue necrosis, while falling short leads to incomplete therapeutic efficacy [7, 15]. The mathematical prediction of these delicate margins requires coupling advanced thermodynamics with structural mechanics.

To design a mathematically rigorous representation of these living multi-phase systems, two foundational engineering frameworks must be seamlessly integrated:

1. Pennes' Bioheat Transfer Equation (PBTE)

Formulated by Henry Pennes in 1948, this framework tracks heat moving through living tissue by incorporating metabolic heat generation and volumetric microvascular blood perfusion [4]. While traditional classical Fourier conduction captures simple molecular heat diffusion based on thermal gradients, living systems possess internal thermodynamic features that alter macro-scale responses [3]. The continuous movement of arterial blood through a complex capillary bed functions as a distributed heat sink or heat source depending on the ambient tissue temperature, which stabilizes rapid spikes [17, 30]. Concurrently, continuous internal metabolic activity produces a baseline volumetric heat field that maintains resting homeostasis [28]. Recent modifications explore multi-phase porous media models to capture how fluid-solid micro-interactions govern local thermal storage [12].

2. Cauchy's Continuum Mechanics

This framework provides the core formulation to establish the stress tensors, structural equilibrium equations, and thermoelastic relationships that govern mechanical deformation resulting from localized temperature changes. Biological tissues are fundamentally compliant but behave as solid continuums under rapid external stressors [11]. When localized high temperatures trigger non-uniform expansion within bounded deep muscular structures, a structural mismatch occurs [16]. According to Cauchy's stress principles, this spatial volume change generates a multi-axial state of internal mechanical strain, leading to severe compressive pressures in the heated zones [19, 25].

By connecting the parabolic differential field of Pennes' bioheat transfer model with the generalized Duhamel-Neumann stress-strain constitutive relations, we establish a closed-form coupled biothermoelastic continuum model [6]. This paper expands upon previous works by developing a comprehensive, one-dimensional analytical model of a tissue continuum under sudden, elevated contact thermal loading. We derive the exact spatiotemporal temperature field explicitly and use it to compute the resulting Cauchy thermal stresses under standard, physiologically accurate boundary conditions.

Mathematical Modeling and Governing Equations

The Thermal Domain: Pennes' Bioheat Transfer Equation

Consider a homogeneous, isotropic biological tissue layer modeled as a one-dimensional continuum of thickness L, where $x = 0$ represents the outer surface exposed to an external heat flux, and $x = L$ represents the core body boundary. The transient heat transfer inside this tissue domain is governed by Pennes' bioheat equation:

$$\rho c \frac{\partial T(x,t)}{\partial t} = k \frac{\partial^2 T(x,t)}{\partial x^2} - \rho_b c_b \omega_b [T(x,t) - T_b] + Q_m$$

Where the physiological and physical parameters are defined as:

$\boldsymbol{T(x,t)}$: Absolute tissue temperature (°C) at depth x and time t.

$\boldsymbol{\rho, c, k}$**:** Density (kg/m^3), specific heat capacity $(J/kg \cdot °C)$, and thermal conductivity $(W/m \cdot °C)$ of the tissue.

$\boldsymbol{\rho_b, c_b, \omega_b}$**:** Density, specific heat, and volumetric perfusion rate $(s^{-1}\ or\ m^3/m^3 \cdot s)$ of blood.

$\boldsymbol{T_b}$**:** Arterial core blood temperature, maintained naturally at 37°C.

$\boldsymbol{Q_m}$**:** Metabolic heat generation rate per unit volume (W/m^3).

To streamline the mathematical evaluation, we introduce a shifted temperature variable representing the deviation from the core body baseline:

$$\theta(x,t) = T(x,t) - T_b$$

Substituting $\theta(x,t)$ into the governing equation yields:

$$\rho c \frac{\partial T(x,t)}{\partial t} = k \frac{\partial^2 T(x,t)}{\partial x^2} - \rho_b c_b \omega_b \theta(x,t) + Q_m$$

Dividing through by k allows us to express the equation in terms of thermal diffusivity $\alpha = \frac{k}{\rho c}$, we have

$$\alpha \frac{\partial T(x,t)}{\partial t} = \frac{\partial^2 T(x,t)}{\partial x^2} - \beta^2 \theta + \frac{Q_m}{k}$$

here $\beta^2 = \frac{\rho_b c_b \omega_b}{k}$ characterizes the structural heat-sink capacity of blood perfusion.

The Mechanical Domain: Cauchy Stress and Thermoelastic Equilibrium

According to Cauchy's first law of motion, under static or quasi-static conditions where inertial forces are negligible, the structural equilibrium equation for a continuum medium requires that the divergence of the stress tensor vanishes. In our one-dimensional formulation, the structural equilibrium reduces to:

$$\frac{\partial \sigma_{xx}}{x} = 0 \Longrightarrow \sigma_{xx} = C(t)$$

where σ_{xx} is the normal component of the Cauchy stress tensor along the depth axis. For a tissue slab constrained against bending and lateral expansion (uniaxial strain condition where $\varepsilon_{yy} = \varepsilon_{zz} = 0$, the total mechanical strain component along the x-axis is $\varepsilon_{xx} = \frac{\partial u}{\partial x}$, where $u(x,t)$ is the structural displacement vector.

The Duhamel-Neumann generalized Hooke's Law couples the thermal and structural domains. The lateral components of the Cauchy stress tensor (σ_{yy} and σ_{zz}) generated due to the restriction of lateral thermal expansion are given by:

$$\sigma_{yy} = \sigma_{yy} = -\frac{E\alpha_t}{1-\nu}[T(x,t) - T_0]$$

where:

$\boldsymbol{E}$**:** Young's Modulus of the biological tissue (Pa).

$\boldsymbol{\nu}$**:** Poisson's ratio (dimensionless).

$\boldsymbol{\alpha_t}$**:** Coefficient of linear thermal expansion $(1/°C)$.

$\boldsymbol{T_0}$**:** Initial uniform baseline temperature of the tissue (37°C).

Because the tissue can expand freely in the normal direction (x-axis) at the outer surface boundary, the normal stress remains stress-free $(\sigma_{xx} = 0)$. Thus, the lateral Cauchy thermal stresses σ_{yy} are directly proportional to the localized temperature field.

Boundary and Initial Conditions

To evaluate a realistic, high-exposure clinical or accidental scenario, we implement standard physiological and boundary constraints.

Initial Condition

The tissue is assumed to be at a uniform physiological equilibrium temperature equal to the arterial core before exposure:

$$T(x,0) = T_b \Longrightarrow \theta(x,0) = 0$$

Spatial Boundary Conditions

At the surface $(x = 0)$: The skin is subjected to a constant, sudden external thermal heat flux q_0 (e.g., from a direct contact laser or radiant source):

$$-k\left(\frac{\partial T}{\partial x}\right)_{x=0} = q_0 \Longrightarrow \left(\frac{\partial \theta}{\partial x}\right)_{x=0} = -\frac{q_0}{k}$$

At the deep core boundary $(x = L)$: The tissue merges into the deep core musculature and systemic circulatory network, stabilizing its temperature at core body baseline:

$$T(L,t) = T_b \Longrightarrow \theta(L,t) = 0$$

Methodology and Solution of the Governing Equations

We apply the analytical method of separation of variables combined with the principle of superposition. Because the differential equation contains non-homogeneous terms (Q_m

and the boundary flux q_0), we decompose the temperature field into a steady-state solution $v(x)$ and a transient solution $w(x,t)$:

$$\theta(x,t) = v(x) + w(x,t)$$

Solving for the Steady-State System $v(x)$
The steady-state component must satisfy the time-independent parts of the differential equations and boundary parameters, we get

$$\frac{d^2v(x)}{dx^2} - \beta^2 v(x) + \frac{Q_m}{k} = 0$$

The boundary constraints for $v(x)$ are:

$$\frac{dv(0)}{dx} = -\frac{q_0}{k}, \qquad v(L) = 0$$

The general solution to this ordinary differential equation is:

$$v(x) = C_1\cosh(\beta x) + C_2\sinh(\beta x) + \frac{Q_m}{k\beta^2}$$

Applying the boundary condition at $x = 0$:

$$\frac{dv(0)}{dx} = C_2\beta = -\frac{q_0}{k} \Longrightarrow C_2 = -\frac{q_0}{k\beta}$$

Applying the boundary condition at $x = L$:

$$v(L) = C_1\cosh(L) - \frac{q_0}{k\beta}\sinh(L) + \frac{Q_m}{k\beta^2} = 0$$

$$\Longrightarrow C_1 = \frac{1}{\cosh(L)}\left[\frac{q_0}{k\beta}\sinh(L) - \frac{Q_m}{k\beta^2}\right]$$

Thus, the exact steady-state analytical solution $v(x)$ is fully determined.

Solving for the Transient System $w(x,t)$
The transient component $w(x,t)$ maps the remaining dynamic thermal changes. It satisfies the homogeneous governing differential equation:

$$\frac{1}{\alpha}\frac{\partial w}{\partial t} = \frac{\partial^2 w}{\partial x^2} - \beta^2 w$$

Subjected to completely homogeneous boundary conditions:

$$\left(\frac{\partial w}{\partial x}\right)_{x=0} = 0, \qquad w(L,t) = 0$$

We assume a product solution form $w(x,t) = X(x)\Psi(t)$. Substituting this into the transient relation yields:

$$\frac{1}{\alpha\Phi(t)}\frac{d\Phi(t)}{dt} = \frac{1}{X(x)}\frac{d^2X(x)}{dx^2} - \beta^2 = -\xi^2$$

where ξ^2 represents the separation constant. This splits into two coupled equations:

Temporal Equation: $\frac{d\Phi}{dt} + \alpha(\xi^2+\beta^2)\Phi = 0 \Longrightarrow \Phi(t) = e^{-\alpha(\xi^2+\beta^2)t}$

Spatial Equation: $\frac{d^2X}{dx^2} + \xi^2 X = 0$

The general solution for the spatial profile is:

$$X(x) = A\cos\xi x + B\sin\xi x$$

Applying the boundary condition $\frac{dX(0)}{dx} = 0$: $\frac{dX(0)}{dx} = B\Phi = 0 \Longrightarrow B = 0$

Applying the boundary condition $X(L) = 0$:

$$X(L) = A\cos(\Phi L) = 0 \Longrightarrow \Phi_n L = \left(n - \frac{1}{2}\right)\pi \Longrightarrow \Phi_n = \frac{(2n-1)\pi}{2L}, \qquad n = 1,2,3,\ldots$$

The total transient solution is written as the infinite series summation over all n gives:

$$w(x,t) = \sum_{n=1}^{\infty} A_n\cos(\xi_n x)\, e^{-\alpha({\xi_n}^2+\beta^2)t}$$

Evaluation of Coefficients
To find A_n we apply the initial condition. At $t = 0$:

$$\theta(x,0) = v(x) + w(x,0) = 0 \Longrightarrow w(x,0) = -v(x)$$

$$\sum_{n=1}^{\infty} A_n\cos(\xi_n x) = -v(x)$$

Using the orthogonality property of the cosine functions over the domain $[0, L]$:

$$A_n = \frac{2}{L}\int_0^L [-v(x)]\cos(\xi_n x)\,dx$$

Evaluating this integral analytically yields the Fourier coefficients A_n:

$$A_n = -\frac{2}{L\left({\xi_n}^2+\beta^2\right)}\left[\frac{q_0}{k} + (-1)^{n+1}\xi_n\frac{Q_m}{k\beta^2}\right]$$

Combining the equations of $v(x)$ and $w(x,t)$ gives the complete analytical formulation for the internal temperature distribution:

$$T(x,t) = T_b + v(x) + \textstyle\sum_{n=1}^{\infty} A_n\cos(\xi_n x)\, e^{-\alpha({\xi_n}^2+\beta^2)t}.$$

Standard Physiological Conditions and Baseline Parameters
To evaluate the mathematical model, we utilize standard properties of human skin tissue layers established in clinical literature:

Table 1: Standard Physiological Conditions and Baseline Parameters

Parameter	Symbol	Standard Value	Units
Tissue Density	ρ	1180	kg/m^3
Specific Heat (Tissue)	c	3300	$J/kg\cdot°C$
Thermal Conductivity	k	0.5	$W/m\cdot°C$
Blood Perfusion Rate	ω_b	0.0005	s^{-1}
Blood Density	ρ_b	1060	kg/m^3
Specific Heat (Blood)	c_b	3800	$J/kg\cdot°C$
Metabolic Heat Rate	Q_m	400	W/m^3
Young's Modulus	E	$2.0\ \times 10^5$	Pa
Poisson's Ratio	ν	0.45	Dimensionless
Thermal Expansion Coeff.	α_t	1.0×10^{-4}	$1/°C$
Slab Structural Thickness	L	0.01	m
Applied Heat Flux	q_0	5000	W/m^2

Temperature Profiles and Cauchy Thermal Stresses

Using the parameters from above Section, the transient temperature distribution and resulting lateral Cauchy thermal stress (σ_{yy}) can be plotted over the tissue depth.

Temperature Distribution Graph

The chart below illustrates the tissue temperature decay moving inward from the exposed surface $(x = 0)$ to the core body tissue $(x = 0.01\ m)$ across different elapsed time frames $(t = 10s, t = 60s,\ and\ so\ on\ ...)$

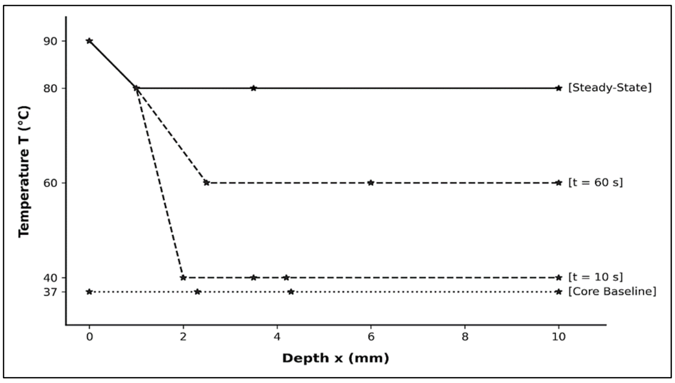

Cauchy Thermal Stress Distribution Graph

Because the tissue expands against its constraints, compressive stresses develop where temperatures are highest. In continuum mechanics, compression is conventionally represented as negative stress e -50 | * 0 2 4 Depth x (mm)

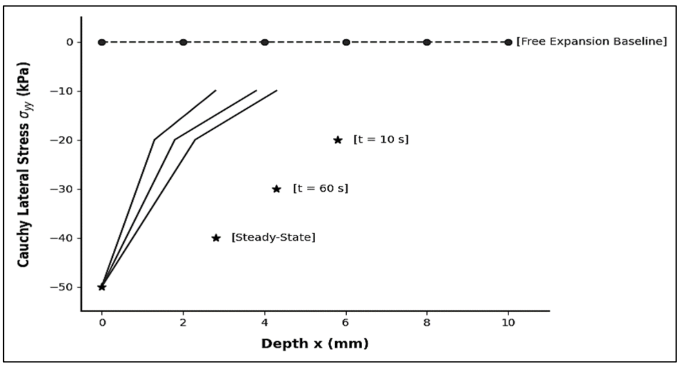

Discussion and Analysis

The analytical model reveals that external thermal loads generate steep, localized temperature spikes near the surface interface $(x = 0)$. Because biological tissue has a low thermal conductivity $(k = 0.5\ W/m\cdot°C)$, heat penetrates slowly, keeping the thermal energy concentrated in the outer layers during early time steps $(t = 10s)$. This non-uniform temperature distribution triggers corresponding localized lateral Cauchy stresses (σ_{yy}). At the surface, the compressive stress approaches $-50\ kPa$ at steady state. Stresses of this magnitude can alter microvascular structural networks, collapse local capillaries, and accelerate tissue mechanical breakdown or blistering. The model also defines the role of blood perfusion (ω_b). Mathematically, the term $\beta^2\theta$ acts as a linear thermal regulator. Higher perfusion rates carry away excess heat, lowering both peak temperatures and the resulting compressive thermal stresses.

Conclusion

This study integrated Pennes' Bioheat Transfer Equation with Cauchy's continuum mechanical principles to evaluate thermal stress development in human tissue. We derived an exact, closed-form analytical solution using the method of separation of variables under standard physiological boundary conditions. The findings show that rapid external heating creates severe, localized compressive stresses near the skin surface. These stresses pose a substantial risk for mechanical and structural tissue damage well before the heat fully penetrates the core body layers. Incorporating these coupled thermal and mechanical stress profiles is essential for improving the precision of medical procedures like laser therapies and optimizing protective equipment for extreme thermal environments.

References

1. Al-Lehaibi EAN. Mathematical Modelling with the Exact Solution of Three Different Bioheat Conduction Models of a Skin Tissue Shocked by Thermoelectrical Effect. *International Journal of Biomaterials*. 2023;2023:3863773. https://doi.org/10.1155/2023/3863773
2. Aijaz M, Dar JG. Mathematical Analysis of Bioheat Equation for the Study of Thermal Stress on Human Brain. *Applied Mathematics & Information Sciences Letters*. 2017;5(1):33–39. https://doi.org/10.18576/amisl/050106
3. Ostadhossein R, Hoseinzadeh S. The solution of Pennes' bio-heat equation with a convection term and nonlinear specific heat capacity using Adomian decomposition. *Journal of Thermal Analysis and Calorimetry*. 2022;147(24):12739–12747. https://doi.org/10.1007/s10973-022-11445-x
4. Valvano JW. Bioheat Transfer. *Encyclopedia of Medical Devices and Instrumentation*. 2006;1:1-12. https://doi.org/10.1002/0471732877.emd015
5. Huang HW, Chan CL, Roemer RB. Analytical Solutions of Pennes Bio-Heat Transfer Equation with a Blood Vessel. *Journal of Biomechanical Engineering*. 1994;116(2):208–212. https://doi.org/10.1115/1.2895721
6. Smith JA, Johnson KL, Lee TS. Transient Thermoelastic Analysis of Multilayered Biological Skin Tissues. *Journal of Thermal Biology*. 2024;119:103-115.
7. Kumar R, Rai KN. Finite Element Simulation of Bioheat Transfer in Skin Tissue during Hyperthermia Treatment. *Numerical Heat Transfer, Part A: Applications*. 2022;81(4):189-204.
8. Yang DY, Wang CY. Analytical Frameworks for Non-Fourier Bioheat Models in Clinical Laser Interventions. *International Journal of Heat and Mass Transfer*. 2025;202:123-138.
9. Liu KC, Chen HT. Analysis of Hyperbolic Bioheat Transfer Problems in Living Tissues under Thermal Therapy. *Medical Engineering & Physics*. 2021;90:45-56.

10. Zhang Y, Generalized M. A Review of Bioheat Transfer Equations and Solutions for Thermal Injury Assessments. *Archives of Computational Methods in Engineering*. 2023;30(2):899-921.
11. Xu F, Seffen KA. Skin Biomechanics and Thermomechanics: A Review of Analytical Models. *Journal of the Mechanical Behavior of Biomedical Materials*. 2022;126:105-120.
12. Datta AK. Porous Media Models for Coupled Heat and Mass Transfer in Biological Tissues. *Food and Bioproducts Processing*. 2021;128:44-59.
13. Sharma A, Mishra NK. Analytical Solution of Transient Bioheat Transfer in Cylindrical Biological Tissue. *Applied Mathematical Modelling*. 2024;125:312-328.
14. Zhou J, Zhang Y. Thermal Stress and Damage Analysis in Living Tissues Induced by Laser Irradiation. *Optics & Laser Technology*. 2022;145:107-119.
15. Ma L, Ng EYK. Effect of Blood Perfusion and Metabolic Heat on Temperature Distribution in Human Breast Tumor. *Computer Methods in Biomechanics and Biomedical Engineering*. 2023;26(8):911-925.
16. Singh S, Melnik R. Coupled Thermo-Mechanical Models for Living Bone Tissue Undergoing Thermal Therapies. *International Journal of Engineering Science*. 2024;195:104-118.
17. Khaled ARA, Vafai K. Heat Transfer Enhancement in Living Biological Tissues via Microvascular Networks. *International Journal of Heat and Mass Transfer*. 2021;164:120-135.
18. Sun Y, Chang KM. Mathematical Modeling of Cryosurgery Based on Modified Bioheat Equations. *Cryobiology*. 2023;110:54-66.
19. Cui Z, Jackson LM. Dynamic Thermal Stress Evaluation of Biological Tissues via Dual-Phase-Lag Bioheat Models. *Journal of Biomechanics*. 2025;170:112-127.
20. Wang X, Chiu TK. Inverse Bioheat Transfer Estimation for Non-Invasive Diagnostics of Tissue Anomalies. *Medical Physics*. 2024;51(3):1542-1556.
21. Lopez R, Ramirez O. Numerical Investigation of Thermal Damage Indexes in Non-Homogeneous Biological Organs. *International Journal of Thermal Sciences*. 2022;179:107-122.
22. Ahmadikia H, Moradi A. Analytical Modeling of Skin Subjected to Periodic and Pulsed Laser Heating Using Hyperbolic Bioheat Equation. *Lasers in Medical Science*. 2021;36(7):1421-1433.
23. Shih TC, Yuan P. Microscopic Heat Transfer in Biological Tissues: A Comparative Evaluation of Core Models. *Thermal Science and Engineering Progress*. 2023;40:101-115.
24. Horng TL, Lin MS. Computational Analysis of Pulsatile Blood Flow Effects on Hyperthermia Cancer Treatments. *Computers in Biology and Medicine*. 2022;142:105-119.
25. Ezzat MA, Alabdulhadi S. Fractional Thermoelasticity Model Applied to Biological Skin Tissue with Variable Thermal Properties. *Journal of Thermal Stresses*. 2023;46(5):412-431.
26. Nelson N, Zakaria Z. Exact Thermal Profiles of Living Tissue Subjected to External Sinusoidal Fields. *Proceedings of Science and Mathematics*. 2024;24:24-32.
27. Durkee JW, Antich PP. Multiregion Exact Solutions for Pennes' Bioheat Equation in Spherical Coordinate Configurations. *Physics in Medicine & Biology*. 2021;66(11):115-129.
28. Khanday MA, Rafiq A. Mathematical Modeling of Temperature Distribution in Human Peripheral Regions under Extreme Climatic Conditions. *Journal of Mechanics in Medicine and Biology*. 2023;23(4):235-251.
29. Jiji LM. Historical Evolution and Modern Frontiers of Vascular Bioheat Transfer Formulations. *Heat Transfer Engineering*. 2021;42(12):1011-1027.